Paraspeckles are subpopulation-specific nuclear bodies that are not essential in mice

Shinichi Nakagawa,[1,2] Takao Naganuma,[3] Go Shioi,[4] and Tetsuro Hirose[3]

[1]RNA Biology Laboratory, RIKEN Advanced Science Institute, 2-1 Hirosawa, Saitama 351-0198, Japan
[2]PRESTO, Japan Science and Technology Agency, Kawaguchi-shi, Saitama 332-0012, Japan
[3]Functional RNomics Team, Biomedicinal Information Research Center, National Institute of Advanced Industrial Science and Technology (AIST), 2-4-7 Aomi, Koutou, Tokyo 135-0064, Japan
[4]Laboratory for Animal Resources and Genetic Engineering, RIKEN Center for Developmental Biology, 2-2-3 Minatojima Minami, Chuou-ku, Kobe 650-0047, Japan

Nuclei of higher organisms are well structured and have multiple, distinct nuclear compartments or nuclear bodies. Paraspeckles are recently identified mammal-specific nuclear bodies ubiquitously found in most cells cultured in vitro. To investigate the physiological role of paraspeckles, we examined the in vivo expression patterns of two long noncoding RNAs, NEAT1_1 and NEAT1_2, which are essential for the architectural integrity of nuclear bodies. Unexpectedly, these genes were only strongly expressed in a particular subpopulation of cells in adult mouse tissues, and prominent paraspeckle formation was observed only in the cells highly expressing NEAT1_2. To further investigate the cellular functions of paraspeckles, we created an animal model lacking NEAT1 by gene targeting. These knockout mice were viable and fertile under laboratory growth conditions, showing no apparent phenotypes except for the disappearance of paraspeckles. We propose that paraspeckles are nonessential, subpopulation-specific nuclear bodies formed secondary to particular environmental triggers.

Introduction

The nuclei of higher eukaryotes are well organized and are composed of distinct nuclear bodies or compartments that contain groups of proteins involved in specific nuclear processes (Platani and Lamond, 2008; Zhao et al., 2009). Although the functional significance or physiological relevance of these nuclear compartments remains to be elucidated, the ordered nuclear structures of higher eukaryotes are speculated to be essential for the complex regulation of gene expression (Platani and Lamond, 2008; Zhao et al., 2009), and growing evidence implicates active involvement of non–protein-coding RNAs in the formation and dynamics of these nuclear structures (Prasanth and Spector, 2007).

Paraspeckles are recently identified nuclear bodies that contain paraspeckle protein (PSP) 1/Pspc1, PSP2/Rbm14, p54[nrb]/Nono, and PSF/Sfpq (Fox et al., 2002; Prasanth et al., 2005), and are usually detected as a variable number of discrete dots found in close proximity to nuclear speckles (Bond and Fox, 2009).

Under electron microscopy, the nuclear body is reminiscent of previously identified structures referred to as interchromatin granule–associated zones (Visa et al., 1993; Souquere et al., 2010). Recently, a bioinformatics approach identified two long noncoding RNAs, nuclear-enriched abundant transcript (NEAT) 1 and 2 (Hutchinson et al., 2007), which are exclusively localized to paraspeckles and nuclear speckles, respectively (Hutchinson et al., 2007; Chen and Carmichael, 2009; Clemson et al., 2009; Sasaki et al., 2009; Sunwoo et al., 2009). Importantly, depletion of NEAT1 by antisense oligonucleotides leads to disintegration of paraspeckles, suggesting that this noncoding RNA serves as a structural component (Chen and Carmichael, 2009; Clemson et al., 2009; Sasaki et al., 2009; Sunwoo et al., 2009). The NEAT1 locus generates short and long transcripts from the same promoter, which have previously been identified as MENε (NEAT1_1) and MENβ (NEAT1_2), respectively (Guru et al., 1997). Because specific depletion of NEAT1_2 leads to disruption of

The Rockefeller University Press $30.00
J. Cell Biol. Vol. 193 No. 1 31–39
www.jcb.org/cgi/doi/10.1083/jcb.201011110

JCB 31

THE JOURNAL OF CELL BIOLOGY

paraspeckles (Sasaki et al., 2009), NEAT1_1 alone cannot induce paraspeckle formation. On the other hand, overexpression of NEAT1_1 increases the number of paraspeckles in the cells expressing NEAT1_2 (Clemson et al., 2009), suggesting that NEAT1_1 becomes a rate-limiting factor for paraspeckle formation under certain conditions. In the current model, NEAT1_2 interacts with core paraspeckle proteins PSF and p54^{nrb}, which recruit PSP1 and NEAT1_1 and other associating molecules to the periphery of paraspeckles (Sasaki et al., 2009; Souquere et al., 2010).

The functional implications of paraspeckles come from a study of the paraspeckle-localizing RNA CTN-RNA, an alternatively spliced form of the cationic amino acid transporter mRNA (Prasanth et al., 2005). The 3′ untranslated region of CTN-RNA contains inverted retrotransposon insertions that form intra-molecular double-stranded RNAs (Prasanth et al., 2005) whose structure is recognized by adenosine deaminase (ADAR), and it is A-to-I edited (Nishikura, 2010). The hyperedited CTN-RNA is particularly enriched in paraspeckles, which concomitantly leads to suppression of gene expression through nuclear retention mediated by the edited region (Prasanth et al., 2005). It has been thus proposed that paraspeckles regulate the expression of hyper-edited transcripts by tethering them within the nuclear bodies (Bond and Fox, 2009; Chen and Carmichael, 2010). The inverted insertions of retrotransposon are not specific to CTN-RNA and are commonly found in the untranslated regions of a variety of mRNAs transcribed from mammalian genomes (Chen et al., 2008; Faulkner et al., 2009), suggesting that the expression of these A-to-I edited transcripts is also potentially suppressed by the nuclear retention mechanism. Interestingly, paraspeckles are absent in human embryonic stem cells, suggesting that paraspeckle-mediated nuclear retention is biologically regulated under certain developmental contexts (Chen and Carmichael, 2009). However, all of the functional analyses have been limited to cultured cells, and their physiological relevance at the level of individual animals remains to be elucidated.

To gain insight into the function of paraspeckles in an animal model, we generated a knockout mouse and found that the mice were viable and fertile, despite the complete lack of paraspeckles in these animals. We propose that paraspeckles are dispensable under normal environmental parameters and might become essential under certain stressed conditions.

Results and discussion

NEAT1_1 and NEAT1_2 are expressed in a particular subpopulation of cells in adult mouse organs

To study the function of paraspeckles in an animal model, we initially examined the expression pattern of NEAT1_1 and NEAT1_2 in various adult mouse tissues by in situ hybridization. Because the probe designed to detect NEAT1_1 inevitably hybridizes to NEAT1_2 (Fig. 1 A), we will use the term "NEAT1" hereafter when we mention the signals detected by the probe. Although NEAT1 was widely expressed, strong signals of NEAT1_2 were restricted to a limited subpopulation of

particular cell types (Fig. 1 B, insets; Fig. S1). The dramatically reduced level of NEAT1_2 expression compared with NEAT1 was also confirmed by quantitative RT-PCR (qPCR), although a significant amount of NEAT1_2 was consistently detected by this detection method (Fig. 1 C). In digestive organs such as stomach and intestine, intense NEAT1_2 signals were detected in the most distal regions of the surface epithelium where natural cell loss occurs (Fig. 1 B, insets). We also examined the expression of NEAT1_1 and NEAT1_2 in early embryos and found that most of the cells did not express both of these transcripts, with the exception of a small number of cells in the hindgut and genital ridges (Fig. 1 D).

Paraspeckles are subpopulation-specific nuclear bodies in vivo

A previous study suggested that expression of NEAT1_2, but not NEAT1_1 is a prerequisite for the formation of paraspeckles (Sasaki et al., 2009). Because NEAT1_2 expression was low or absent in most of the cells from the mouse tissues (Fig. 1, B and D; Fig. S1), we speculated that paraspeckles were not ubiquitously formed in vivo. To confirm this, we examined the subcellular localization of paraspeckle markers PSF (Prasanth et al., 2005) and PSP2 (Fox et al., 2002) in the zymogenic glands of the stomach, where strong NEAT1_2 expression was observed in the surface but not in the deep layer of the gastric epithelium (Fig. 2, A and B). In the surface epithelial cells, PSF and PSP2 were concentrated in discrete large foci that completely overlapped with the distribution of NEAT1 and NEAT1_2 (Fig. 2 C). On the other hand, other gastric cells deeper in the epithelium, such as parietal cells, lacked strong NEAT1_2 expression, although weak signals were observed at the putative transcription sites (Fig. 2 D, arrowheads). In these cells, NEAT1 transcripts were diffused from the transcription sites into the nucleoplasm, and the paraspeckle markers were uniformly distributed with some enrichment on the putative NEAT1_2 transcription sites (Fig. 2 D, arrowheads). These data suggested that prominent formation of paraspeckles is observed only in the cells that highly express NEAT1_2. It should be noted that the deep layer of the gastric epithelium expressed a significant amount of NEAT1_2 (Fig. 2 B), which was higher than the expression in mouse embryonic fibroblasts (MEFs) that possess discrete paraspeckles (see Fig. 4, A and B). We occasionally found strong NEAT1_2–expressing cells in the deep layer of the epithelium, which might account for the signals detected by qPCR. Alternatively, NEAT1_2 expression itself might not be sufficient for the paraspeckle formation.

In cells weakly expressing NEAT1_2, the NEAT1 signals were expected to represent mostly NEAT1 distribution. We then compared the signals of NEAT1_1 with another nuclear-retained noncoding RNA, Malat1/NEAT2, which localizes to the nuclear speckles (Hutchinson et al., 2007; Tripathi et al., 2010). Although the signals of NEAT1_1 and Malat1 overlapped to some extent, they essentially occupied distinct nuclear domains (Fig. 2 E), suggesting that NEAT1_1 is not localized to the nuclear speckles. All of these observations suggest that paraspeckles are specialized nuclear bodies found in a restricted subpopulation of cells highly expressing NEAT1_2. Interestingly,
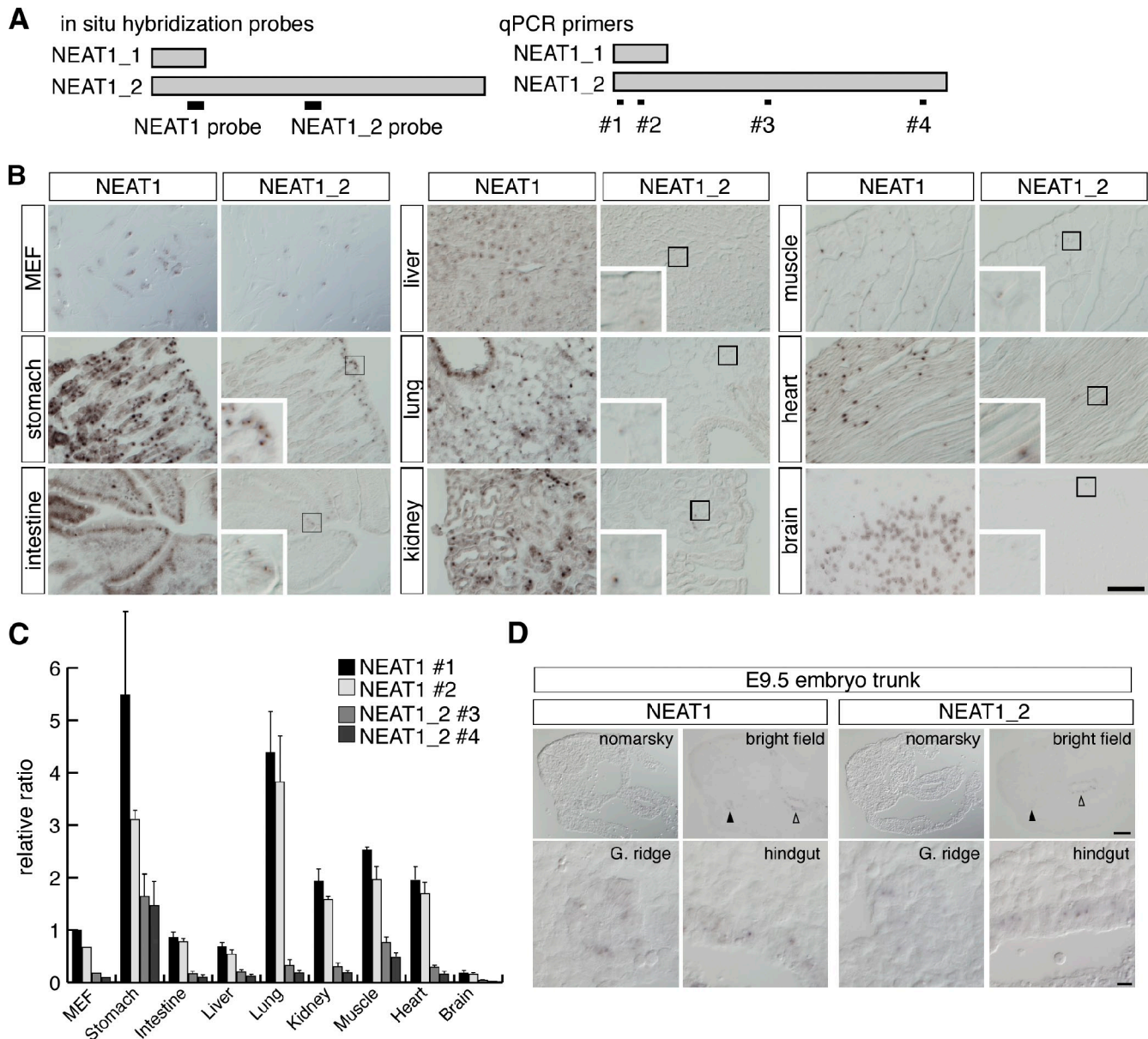
Figure 1. NEAT1_1 and NEAT1_2 are expressed in a particular subpopulation of cells in mouse tissues. (A) Schematic drawing of the position of the probes used for in situ hybridization and primers used for qPCR analysis. (B) Expression of NEAT1 and NEAT1_2 in various adult organs detected by in situ hybridization. Insets show higher magnification images of the region indicated by boxes. (C) qPCR analysis of expression of NEAT1 and NEAT1_2. (D) Expression of NEAT1 and NEAT1_2 in the trunk region of E9.5 embryos. Faint expression is observed in cells in the hindgut (open arrowheads) and genital ridges (arrowheads). Bars, 100 μm.

embryonic cells that normally lack NEAT1 expression up-regulated NEAT1_2 when they were cultured as MEFs as early as 18 h after culturing (Fig. 2 F), resulting in the formation of paraspeckles (Fig. 2 G, arrows). We also found that the expression level of NEAT1 and NEAT1_2 as well as the number of paraspeckles were highly variable between different animals in certain tissues such as liver (Fig. S2).

NEAT1 knockout mice are viable and fertile

To further investigate the physiological role of paraspeckles, we generated knockout mice of NEAT1 by inserting lacZ and poly-adenylation signals immediately downstream of the transcriptional start site (Fig. 3 A). Unexpectedly, the knockout allele was inherited in normal Mendelian ratios (Table I), suggesting that NEAT1 knockout mice are viable and fertile. To confirm the loss of NEAT1 expression in the homozygous animals, we prepared MEFs from E14.5 embryos and examined the expression of NEAT1 and NEAT1_2 by qPCR (Fig. 3 D). Expression of NEAT1 was decreased to $38.5 \pm 5.5\%$ (SD, $n = 2$) and $6 \pm 0.5\%$ (SD, $n = 3$) of the wild-type level in the MEFs prepared from heterozygous and homozygous mutant mice, respectively (Fig. 3 D). On the other hand, we could not detect NEAT1_2 expression (Fig. 3 D). We also confirmed the dramatic decrease of NEAT1 expression and complete loss of NEAT1_2 expression on histological sections by in situ hybridization (Fig. 3 E). We could not see any differences in body weight between the wild-type and knockout adult mice (Fig. 3 F).
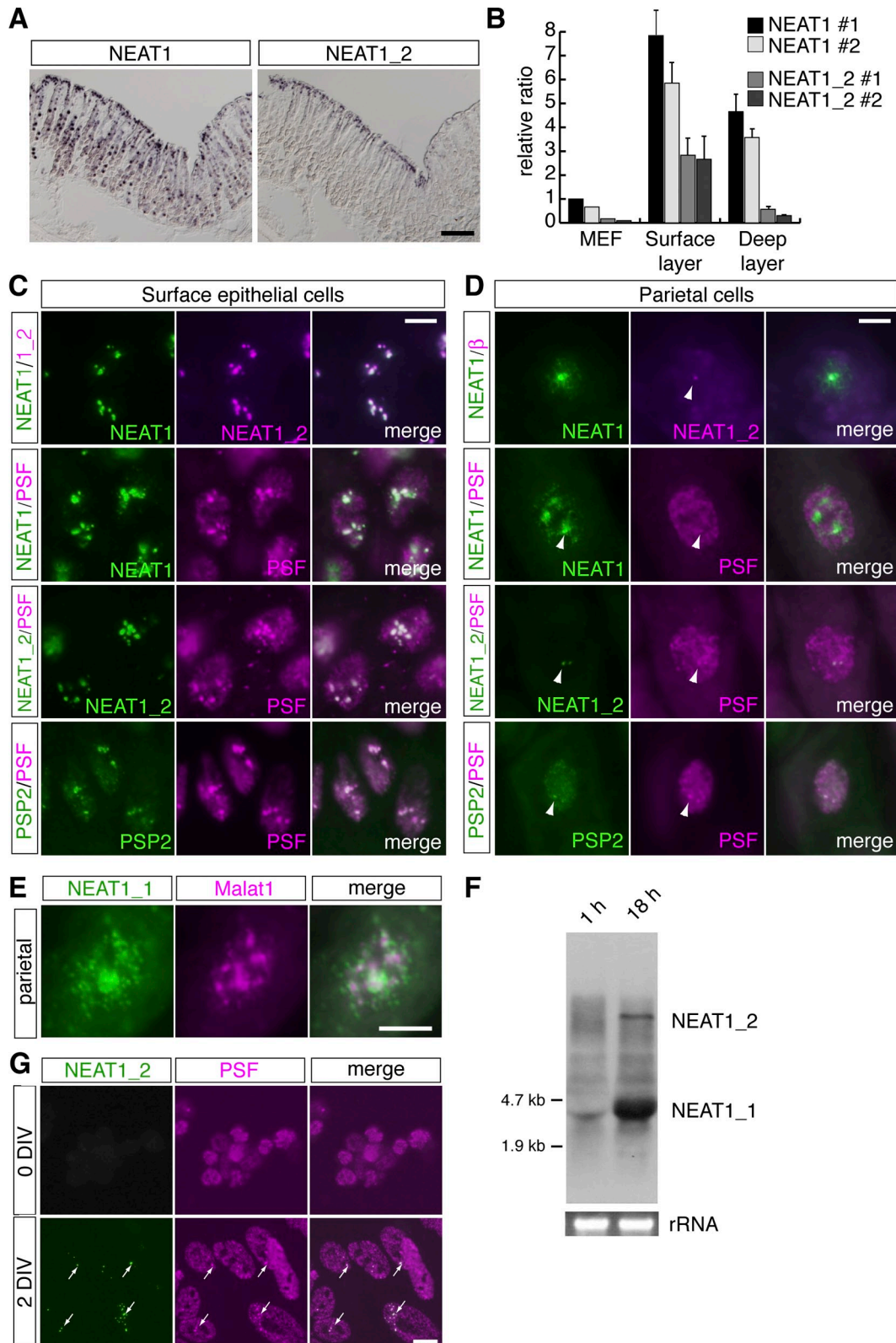
Figure 2. **Paraspeckles are formed only in a small subpopulation of cells expressing NEAT1_2.** (A) Expression pattern of NEAT1 and NEAT1_2 in the zymogenic region of the adult stomach detected by in situ hybridization. NEAT1_2 expression is restricted to the surface epithelial cells facing the lumen of the stomach. (B) qPCR analysis of the expression of NEAT1 and NEAT1_2 in the dissected surface and deep layer of the gastric epithelium. (C and D) Subnuclear distribution of NEAT1, NEAT1_2 detected by FISH, and the paraspeckle marker PSF and PSP2 in the surface epithelial cells (C) and parietal cells (D). Arrowheads in D indicate the putative transcription sites of NEAT1_2. (E) Different expression of NEAT1_1 and Malat1 in parietal cells that lack expression of NEAT1_2. (F) Induction of NEAT1 expression in cultured MEFs. (G) Paraspeckle formation is rapidly induced in MEFs cultured in vitro (DIV, days in vitro). Bars: (A) 100 µm; (C, D, and G) 10 µm; (E) 5 µm.
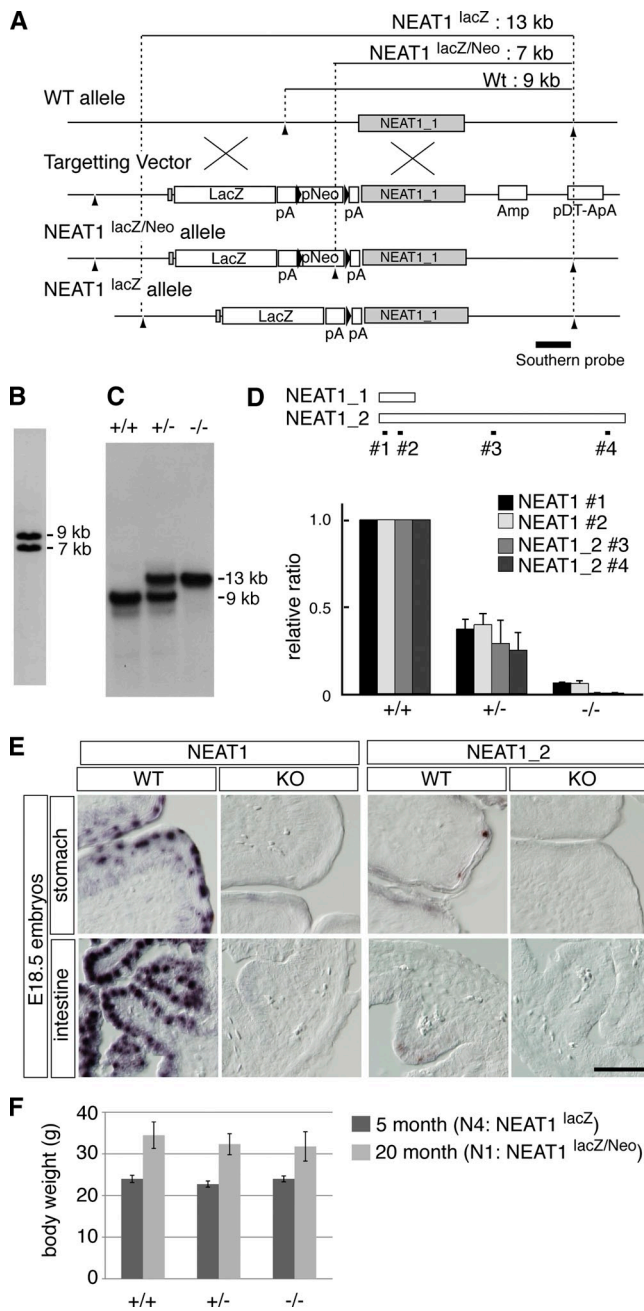
Figure 3. **Generation of NEAT1 knockout mouse.** (A) Targeting strategy for disruption of the NEAT1 gene. Arrowheads indicate SphI restriction sites, and black triangles indicate the FRT sequences flanking the Neo cassette. (B) Southern blot analysis of SphI-digested DNA from embryonic stem cells that underwent homologous recombination. (C) Southern blot analysis of SphI-digested tail DNA from of NEAT1^{lacZ} mice. (D) Quantitative PCR analysis of NEAT1 and NEAT1_2 transcripts. (E) In situ hybridization of NEAT1 and NEAT1_2 in stomach and intestine of E18.5 embryos. Bar, 100 µm. (F) Body weight of female littermates (n = 3 for each genotype).

Paraspeckle formation is not observed in the cells lacking NEAT1 expression

We then examined if paraspeckles are formed in MEFs prepared from the NEAT1 knockout mice. As previously reported, PSF was concentrated in discrete foci that coincided with NEAT1 signals in MEFs from wild-type animals. On the other hand, PSF foci were completely absent in the MEFs derived from

knockout embryos (Fig. 4 A). To further confirm the loss of paraspeckles, we transiently introduced PSP1 fused to the fluorescent protein Venus (Sasaki et al., 2009) into these cells and directly observed the fluorescent signals (Fig. 4, B and C). Typically, the PSP1-Venus signal was observed as 5–10 discrete foci with diffuse nucleoplasmic signals in the wild-type MEFs (Fig. 4 B); however, they were evenly distributed in the nucleoplasm of NEAT1 knockout MEFs (Fig. 4 B). Because the transient expression of PSP1-Venus occasionally resulted in abnormal aggregation of overexpressed protein when the expression level was extremely high (Fig. 4 C), we categorized 200 PSP1-Venus–expressing cells into four groups and counted the number of cells in each category: type I cells contained large, round foci; type II cells contained numerous dots scattered throughout the nucleoplasm; type III cells showed typical paraspeckle-like patterns; and type IV cells had uniform signals in the nucleoplasm. In wild-type cells, paraspeckle-like localization of PSP1-Venus was observed in $46.5 \pm 1\%$ (SD, $n = 2$) of the cells, whereas this pattern was observed in only $1.5 \pm 0.4\%$ (SD, $n = 2$) of the cells prepared from NEAT1 knockout mice.

We next examined the subnuclear localization of PSF in adult tissues to confirm the loss of paraspeckles in vivo. For these experiments, we specifically focused on three types of cells: esophageal epithelial cells, forestomach epithelial cells, and surface mucous cells in zymogenic stomach, all of which expressed the highest levels of NEAT1_2 (Fig. 4 D; Fig. S1). In the wild-type cells, formation of paraspeckles was confirmed by prominent accumulation of PSF in discrete foci (Fig. 4 D, left). On the other hand, the paraspeckle marker was evenly distributed throughout the nuclei of the homozygous mice (Fig. 4 D, right), suggesting that paraspeckles were indeed disrupted in the tissues of the NEAT1 knockout mice.

Histological organization of the stomach is apparently normal in NEAT1 knockout mice

Finally, we examined tissue integrity in NEAT1 knockout mice by cell type–specific marker expression (Fig. 5). For this analysis, we again focused on the zymogenic region of the stomach, which strongly expresses both NEAT1_1 and NEAT1_2 and contains multiple cell types clearly distinguished by expression of differentiation markers. In this region, the zymogenic gastric gland mainly consists of three mature epithelial cell types (Lee et al., 1982): surface epithelial cells expressing mucin 5ac (Muc5ac), acid-secreting parietal cells expressing ATP-transporter 4b (Atp4b), and enzyme-secreting zymogenic cells expressing pepsinogen C (Pgc; Fig. 5 B). As mentioned above, NEAT1 were broadly expressed in all three of these cell types, whereas NEAT1_2 was restricted to a subpopulation of surface mucous cells facing the lumen of the stomach (Fig. 4, Fig. 5 A). In the knockout mice, expression of NEAT1_2 was essentially undetectable; however, differentiation of the surface epithelial cells in the knockout mice was normal, judging from the expression of Muc5ac (Fig. 5, A and B). We also evaluated the epithelial organization of the gastric epithelium by examining the expression of E-cadherin, which is strongly expressed in the surface epithelial cells (Shimoyama and Hirohashi, 1991). E-cadherin was properly accumulated at cell–cell junctions in

Table I. **Genotypes of offspring from the NEAT1-knockout mice**

Heterozygotes x Heterozygotes

Father	Mother	Age	+/+	+/−	−/−
NEAT1$^{lacZ/Neo}$ (F1)	NEAT1$^{lacZ/Neo}$ (F1)	E9.5–E17.5	11	22	13
NEAT1$^{lacZ/Neo}$ (F2)	NEAT1$^{lacZ/Neo}$ (F2)	20 mo	15	36	19
NEAT1^{lacZ} (F2)	NEAT1^{lacZ} (F2)	14–15 mo	14	19	14
NEAT1^{lacZ} (F3)	NEAT1^{lacZ} (F3)	11–12 mo	14	19	9
NEAT1^{lacZ} (F4)	NEAT1^{lacZ} (F4)	3–5 mo	7	6	4
		Total	61	102	59

Homozygotes x wild type

Father	Mother	Age	+/+	+/−	−/−
C57BL/6	NEAT1^{lacZ} (N2)	3 mo	0	6	0
NEAT1^{lacZ} (N2)	C57BL/6	3 mo	0	8	0

F1–3, heterozygous mice of F generations 1–3, N2, homozygous mice of N2 generation.
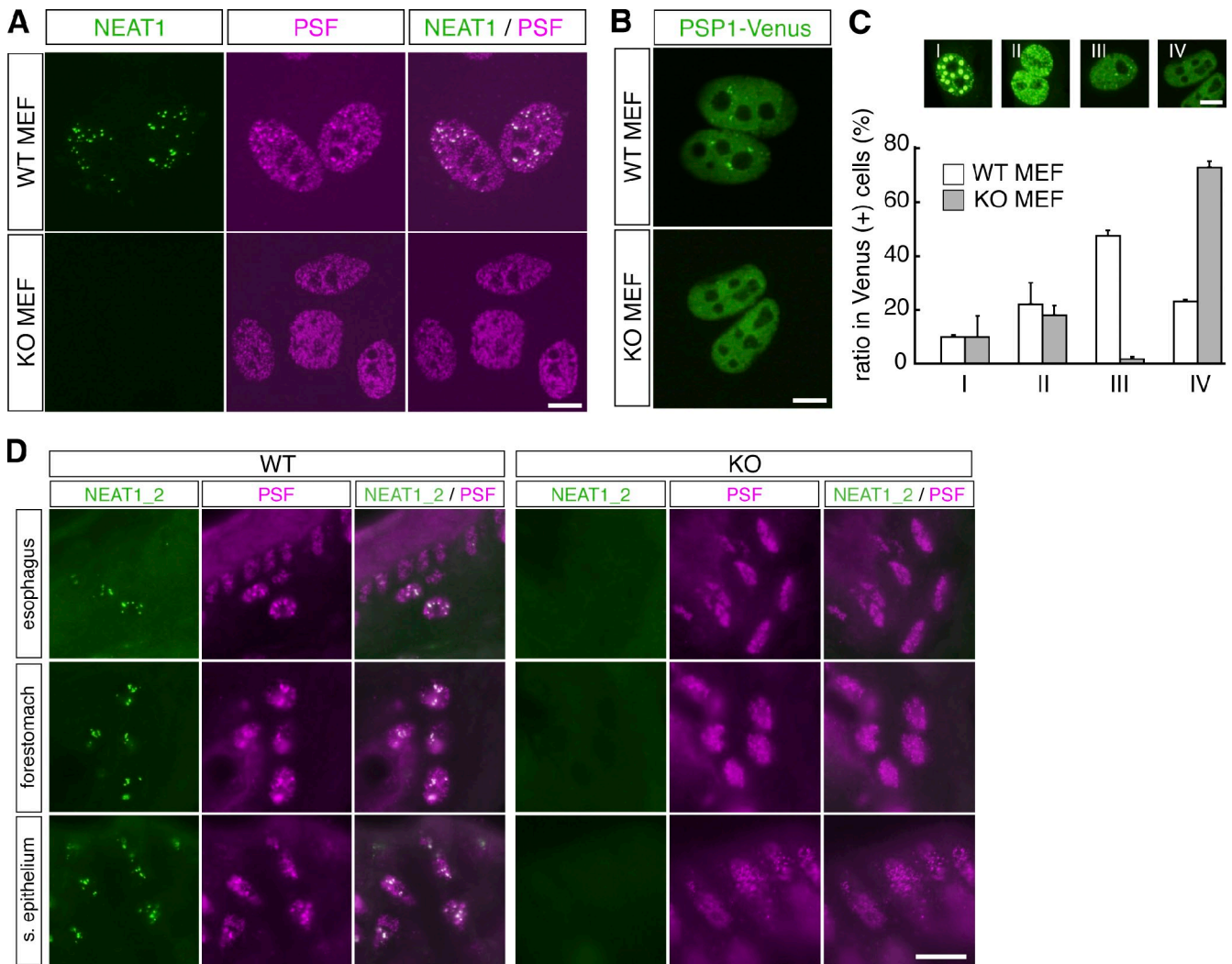

Figure 4. **Paraspeckles are not formed in NEAT1 knockout mice.** (A) Subnuclear localization of NEAT1_2 and the paraspeckle marker PSF in MEFs. The foci of PSF were not observable in MEFs from NEAT1 knockout mice. (B) Typical distribution of PSP1-Venus in MEFs from wild-type (WT) and knockout (KO) mice. The paraspeckle marker accumulated as discrete foci in WT MEFs, but not in knockout MEFs. (C) Quantitative analysis of subnuclear localization of PSP1-Venus in WT and knockout MEFs. Overexpressed PSP1-Venus signals were categorized as types I–IV. Note that typical paraspeckle-like distribution (type III) was rarely observed in knockout MEFs. (D) Loss of punctate signals of paraspeckle marker PSF in epithelial cells of esophagus, forestomach, and surface epithelium (s. epithelium) of zymogenic stomach in the knockout mice. Bars, 10 µm.
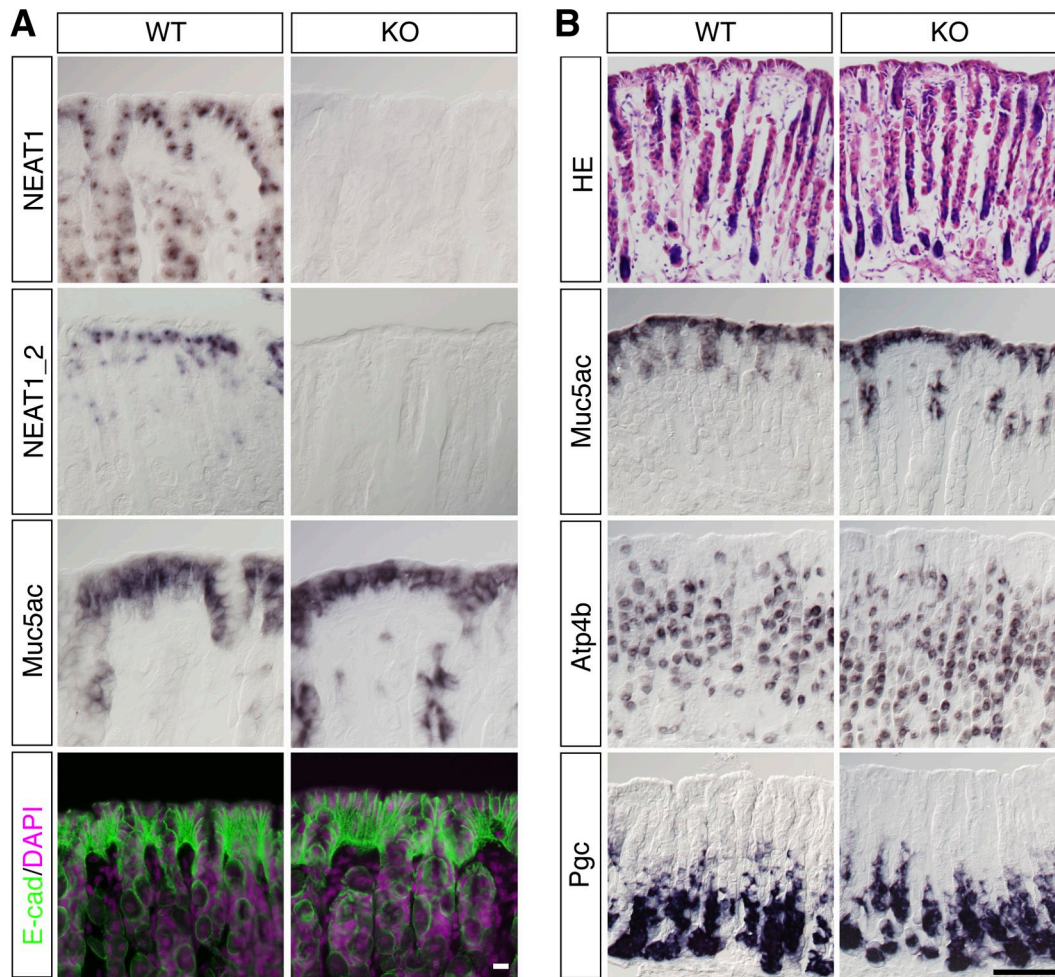
Figure 5. **Normal tissue organization of stomach in NEAT1 knockout mice.** (A) Expression pattern of NEAT1, NEAT1_2, surface epithelial cell marker Muc5ac, and cell–cell junction marker E-cadherin (E-cad) in the zymogenic epithelium in the wild-type and NEAT1 knockout stomach. (B) Normal organization of tissue integrity revealed by histological HE staining and in situ hybridization for Muc5ac, Atp4b, and Pgc, which are expressed in surface mucosa cells, acid-producing parietal cells, and enzyme-producing zymogenic cells, respectively. Bars: (A) 10 µm; (B) 100 µm.

the wild-type and knockout mice (Fig. 5 A), suggesting that epithelial organization is properly maintained in the zymogenic epithelium of NEAT1 knockout mice. Differentiation markers for parietal cells (Atp4b) and zymogenic cells (Pgc) were also appropriately expressed (Fig. 5 B), suggesting that basic histological organization is not affected by the depletion of NEAT1 expression.

Functional relevance of subpopulation-specific formation of paraspeckles

In this study, we showed that paraspeckles are not ubiquitous, but rather they are subpopulation-specific nuclear bodies found in cells highly expressing NEAT1_2. This observation contrasts strikingly with previous reports that paraspeckles are found in all of the cell types examined, except for in human embryonic stem cells (Hutchinson et al., 2007; Chen and Carmichael, 2009; Clemson et al., 2009; Sasaki et al., 2009; Sunwoo et al., 2009). Given that the expression of NEAT1 and subsequent paraspeckle formation were rapidly induced when embryonic cells were cultured on a plastic dish as MEFs, paraspeckle formation might be a natural cellular response to certain changes in the extracellular

environment, reminiscent of the formation of bundled actin stress fibers that can never be observed in fibroblast cells within embryos (Hay, 2005). It is worthwhile to note that the 5′ region of this transcript is induced upon infection with the Japanese encephalitis virus or Rabies virus in the nervous system (Saha et al., 2006). Paraspeckle formation may thus be a cellular response to certain infectious diseases or extracellular stressors, an unnecessary adaptation under normal circumstances. It would be interesting to test if the knockout mice show increased sensitivity to viruses or microbes that induce paraspeckle formation.

Although strong expression of NEAT1_2 was limited to a subpopulation of particular cell types in a restricted region in various tissues, NEAT1_1 was expressed in a much broader spectrum of cell types. In these cells, NEAT1_1 transcripts were detected as a number of small dots widely distributed in the nucleoplasm, which did not coincide with the distribution of the paraspeckle marker PSF. Therefore, the nuclear retention of NEAT1_1 and formation of paraspeckles are independently controlled by a yet-unknown mechanism. As low levels of NEAT1_1 expression were still observed in our knockout mice, we cannot exclude the possibility that NEAT1_1 plays essential

roles in cellular functions independent of paraspeckles by making novel nuclear bodies. Identification of the components of the NEAT1_1 complex may reveal paraspeckle-independent function of this nuclear-retained noncoding RNA.

Collectively, our findings demonstrate that NEAT1_2 expression and subsequent paraspeckle formation are restricted to a small subpopulation of cells in living animals, and a lack of paraspeckles does not lead to obvious phenotypes. It will be particularly important to determine the experimental conditions under which paraspeckles become physiologically essential in order to address the actual function of these nuclear bodies.

Materials and methods

In situ hybridization and immunohistochemistry

Adult mice were anesthetized with pentobarbital and perfused with 4% paraformaldehyde (PFA) in PBS. Dissected tissues were further fixed in 4% paraformaldehyde overnight at 4°C, cryoprotected with 30% sucrose in PBS, and embedded in Tissue-Tek (Sakura). Sections 10 µm thick were collected on PLL-coated glass slides (Matsunami-glass) and processed for in situ hybridization as described previously (Sone et al., 2007). In brief, the slides were refixed with 4% PFA in PBS for 15 min, treated with 0.2 N HCl for 20 min, and subsequently treated with 3 µg/ml proteinase K (PCR grade; Roche) at 37°C for 7 min. After acetylation with 1.5% triethanolamine, 0.25% acetic anhydride, and 0.25% 11 N HCl they were hybridized with DIG- or FITC-labeled probes (1 µg/ml) for 20 h at 55°C in a hybridization buffer (50% formamide, 2x SSC, 1x Denhardt's solution, 5% dextran-sulfate, 10 mM EDTA, and 0.01% Tween 20). After washing twice with a solution containing 50% formamide, 2x SSC, and 0.01% Tween 20 at 55°C for 30 min each, the samples were treated with 10 µg/ml RNase A at 37°C for 1 h in a buffer (0.5 M NaCl, 10 mM Tris, pH 8.0, 1 mM EDTA, and 0.01% Tween 20). They were then sequentially washed with 2x SSC and 0.01% Tween 20 at 55°C for 30 min, with 0.2x SSC and 0.01% Tween 20 at 55°C for 30 min, and finally with Tris-buffered saline (TBS, pH 7.6). Probes were then detected by standard immunohistochemical methods using the antibodies described below. To detect signals with alkaline phosphatase–conjugated secondary antibody, a chromogenic reaction using NBT/BCIP (Roche) was performed in a buffer containing 10% polyvinyl alcohol (Sigma-Aldrich) to increase the spatial resolution. For cultured cells, cells were plated on PLL-coated 8-well camber slides (Laboratory-Tek II chamber slide; Thermo Fisher Scientific) and processed in the same manner as tissue sections. For detection with anti-PSP2 antibody, tissues were fixed for 30 min at 4°C, cryosectioned, and treated with Histo-VT One (Nacalai) according to the manufacturer's instructions. The weak fixation condition was essential to obtain PSP2 signals. Antibodies used were mouse monoclonal anti-PSF antibody (P2860; Sigma-Aldrich), rabbit anti-PSP2 antibody (anti-CoAA: A300-331A, Bethyl Laboratories, Inc.), rat monoclonal anti–E-cadherin (ECCD2) antibody (Shirayoshi et al., 1986), alkaline phosphatase–conjugated sheep anti-DIG antibody (11 093 274 910; Roche), rabbit polyclonal anti-FITC antibody (ab73831; Abcam), Cy3-conjugated goat anti–mouse antibody (AP124C; Millipore), Cy3-conjugated goat anti–rat antibody (AP183C; Millipore), and Alexa Fluor 488–conjugated anti–rabbit antibody (A11029; Invitrogen). Dig- or FITC-labeled RNA probes were prepared using an RNA-labeling mixture (Roche) and T3 and T7 RNA polymerase (Roche) according to the manufacturer's instructions. To prepare templates for the RNA probes, cDNA fragments were amplified using M13 FW and RV primers, and the following EST clones were used as templates: AV089414 for NEAT1, AK009732 for Atp4b, AK160474 for Pgc, and AK008656 for Muc5ac. To generate NEAT1_2 probes, cDNA fragments were amplified using primers provided in the supplemental material using the BAC clone RP23-209P9 as a template, which was subcloned into pCRII (Invitrogen). The fluorescent and DIC images were obtained using an epifluorescent microscope (BX51; Olympus) equipped with a CCD camera (DP70).

Generation of NEAT1 knockout mice

The NEAT1 knockout mouse was generated following protocols described previously (Murata et al., 2004). In brief, DNA fragments were amplified by PCR using the BAC clone RP23-209P9 as a template and subcloned into DT-ApA/LacZ/NeO to generate the targeting vector. The linearized targeting vector was electroporated into TT2 embryonic stem cells (Yagi et al., 1993),

and G418-resistant clones were screened by PCR followed by Southern blot analysis for homologous recombination. Chimeric mice were generated with the recombinant embryonic stem clone and mated with C57BL/6 females to generate heterozygous animals (NEAT1$^{lacZ/Neo}$/+). They were then mated with Gt (ROSA)26So$_r$$^{tm1(FLP1)Dym}$ (The Jackson Laboratory) to flip out the PGK-Neo cassette, and the resultant heterozygous mice (NEAT1^{lacZ}/+) were maintained on the C57BL/6 genetic background. PCR-mediated genotyping was performed using DNAs obtained from adult or embryonic tails. First, DNA was predenatured at 96°C for 1 min, followed by 30 cycles of denaturation at 94°C for 30 s, annealing at 62°C for 30 s, and extension at 72°C for 30 s. The RIKEN accession no. of the NEAT1 knockout mouse is CDB0773K, and detailed information is available at the following address: http://www.cdb.riken.jp/arg/mutant%20mice%20list .html. All the animal protocols were approved by the safety division of RIKEN (#H22-EP056).

Cell cultures

Cells were cultured in a 1:1 mixture of DME (Nissui) and Ham's F12 (Nissui) supplemented with 10% fetal bovine serum (DH10). To prepare MEFs, littermates were obtained by crossing mice from the F4 (NEAT1^{lacZ}/+) generation. Embryonic day 14 (E14) embryos were collected in Ca^{2+}- and Mg^{2+}-free saline-buffered solution with Hepes (HCMF: 10 mM Hepes, pH 7.4) and treated with 0.5% trypsin (1:50; Difco) in HCMF containing 1 mM EDTA at 37°C for 15 min. After addition of an equal amount of DH10, the embryos were dissociated into single cells by mild pipetting, centrifuged, and resuspended in fresh medium. Cells from single embryos were plated into a 6-cm culture dish (Thermo Fisher Scientific). The next day, cells were transferred into 10-cm dishes and further cultured for up to 3 passages with a split ratio of 1:5. For PSP1-Venus transfection, 5 × 10^6 cells were plated into a well of 6-well culture dishes (Thermo Fisher Scientific) and transfected with the plasmid using Effectene reagents (QIAGEN) according to the manufacturer's instructions. 24 h after transfection, cells were plated on 8-well chamber slides (Laboratory-Tek II; Thermo Fisher Scientific) and further cultured for 48 h. The Venus fluorescence images were directly obtained using epifluorescent microscopy after fixation. This was essential for observing the paraspeckle-like PSP1 signals in the cells because conventional permeabilization and subsequent immunohistochemical procedures diminished the paraspeckle localization of PSP1 for unknown reasons.

Quantitative reverse transcription–polymerase chain reaction (qRT-PCR)

qRT-PCR was performed as described previously (Sasaki et al., 2009). In brief, total RNA was prepared from cell culture and mouse tissues using Trizol reagent (Invitrogen). To quantify the expression of NEAT1 and NEAT1_2 in the surface and deep layers of gastric epithelium, the stomach was initially cut into small strips at a width of 0.5 mm using ophthalmic surgery scissors, and further divided into sublayers using sharpened minuten pins on silicon dishes. The total RNA (1 µg) was reverse transcribed using QuantiTect reverse transcription kit (QIAGEN). The primers were designed by Primer3 software (see supplemental material) and purchased from Invitrogen. Aliquots of cDNA were subjected to real-time PCR, performed using a Lightcycler 480 SYBR Green I Master (Roche) according to the manufacturer's protocol. 28S rRNA was used for the normalization control between the samples. The normalization of relative expression of NEAT1 and NEAT1_2 was performed by measuring the values using plasmid DNA that contains full-length NEAT1_2 as a template. The relative expression of NEAT1 in MEF was standardized as 1.

Primers used in this study

Target vector construction/knockout mouse genotyping: Left arm forward (FW), 5'-gaattcgtcgacTGTGGGTCTGTACCACTTGAGTTTCTAGTG-3'; Left arm reverse (RV), 5'-gaattcgcggccgcCTGAGCCCTGAACTGGCCACTGCCTCC-3'; Right arm FW, 5'-gaattcgatatcAGGCAGCCACTAGGATGGGGGT-GCGAG-3'; Right arm RV, 5'-gaattcgtcgacCCATGGTGCAGTGCATCTAG-GCCTAACTAT-3'; Southern probe FW, 5'-CTGCAAACACTGCTCTATGC-3'; Southern probe RV, 5'-GAAATCATGTTAAGGACACTC-3'; embryonic stem PCR check primer FW, 5'-CATCGCCTTCTATCGCCTTCTTGACG-3'; embryonic stem PCR check primer RV, 5'-AGATCATGTTCAGAATACTCCCTTACC-3'; Genotyping PCR knockout FW, 5'-TTGAAGTGGCGAGCGATAC-3'; Genotyping PCR knockout RV, 5'-AGATCCCAGCGGTCAAAAC-3'; Genotyping PCR WT FW, 5'-CTAGTGGTGGGGAGGCAGT-3'; Genotyping PCR WT RV, 5'-AGCAGGGATAGCCTGGTCTT-3'; Quantitative analysis of NEAT1 expression: qPCR NEAT1#1 FW, 5'-TTGGGACAGTGGACGTGTGG-3'; qPCR NEAT1#1 RV, 5'-TCAAGTGCCAGCAGACAGCA-3'; qPCR NEAT1#2 FW, 5'-GATCGGGACCCCAGTGACCT-3'; qPCR NEAT1#2 RV,

5′-AGCTTTCCCCAACACCCACA-3′; qPCR NEAT1_2#3 FW, 5′-AACTGC-TACCCACCGAGATG-3′; qPCR NEAT1_2#3 RV, 5′-TGCTTACACGGCTT-GTTCAG-3′; qPCR NEAT1_2#4 FW, 5′-GCTCTGGGACCTTCGTGACTCT-3′; qPCR NEAT1_2#4 RV, 5′-CTGCCTTGGCTTGGAAATGTAA-3′; Probes for in situ hybridization: NEAT1_2 probe FW, 5′-TATTGGCCAATCACGAGT-3′; NEAT1_2 probe RV, 5′-AAAGCTGCCTGAGGCTCA-3′.

Online supplemental material

Fig. S1 shows that NEAT1 and NEAT1_2 are expressed in a particular population of cells in mouse tissues. Fig. S2 shows variable expression of NEAT1 and NEAT1_2 in the liver of different animals. Online supplemental material is available at http://www.jcb.org/cgi/content/full/jcb.201011110/DC1.

References

Bond, C.S., and A.H. Fox. 2009. Paraspeckles: nuclear bodies built on long non-coding RNA. *J. Cell Biol.* 186:637–644. doi:10.1083/jcb.200906113

Chen, L.-L., and G.G. Carmichael. 2009. Altered nuclear retention of mRNAs containing inverted repeats in human embryonic stem cells: functional role of a nuclear noncoding RNA. *Mol. Cell.* 35:467–478. doi:10.1016/j.molcel.2009.06.027

Chen, L.L., and G.G. Carmichael. 2010. Decoding the function of nuclear long non-coding RNAs. *Curr. Opin. Cell Biol.* 22:357–364. doi:10.1016/j.ceb.2010.03.003

Chen, L.L., J.N. DeCerbo, and G.G. Carmichael. 2008. Alu element-mediated gene silencing. *EMBO J.* 27:1694–1705. doi:10.1038/emboj.2008.94

Clemson, C.M., J.N. Hutchinson, S.A. Sara, A.W. Ensminger, A.H. Fox, A. Chess, and J.B. Lawrence. 2009. An architectural role for a nuclear non-coding RNA: NEAT1 RNA is essential for the structure of paraspeckles. *Mol. Cell.* 33:717–726. doi:10.1016/j.molcel.2009.01.026

Faulkner, G.J., Y. Kimura, C.O. Daub, S. Wani, C. Plessy, K.M. Irvine, K. Schroder, N. Cloonan, A.L. Steptoe, T. Lassmann, et al. 2009. The regulated retrotransposon transcriptome of mammalian cells. *Nat. Genet.* 41:563–571. doi:10.1038/ng.368

Fox, A.H., Y.W. Lam, A.K.L. Leung, C.E. Lyon, J. Andersen, M. Mann, and A.I. Lamond. 2002. Paraspeckles: a novel nuclear domain. *Curr. Biol.* 12:13–25. doi:10.1016/S0960-9822(01)00632-7

Guru, S.C., S.K. Agarwal, P. Manickam, S.E. Olufemi, J.S. Crabtree, J.M. Weisemann, M.B. Kester, Y.S. Kim, Y. Wang, M.R. Emmert-Buck, et al. 1997. A transcript map for the 2.8-Mb region containing the multiple endocrine neoplasia type 1 locus. *Genome Res.* 7:725–735.

Hay, E.D. 2005. The mesenchymal cell, its role in the embryo, and the remarkable signaling mechanisms that create it. *Dev. Dyn.* 233:706–720. doi:10.1002/dvdy.20345

Hutchinson, J.N., A.W. Ensminger, C.M. Clemson, C.R. Lynch, J.B. Lawrence, and A. Chess. 2007. A screen for nuclear transcripts identifies two linked noncoding RNAs associated with SC35 splicing domains. *BMC Genomics.* 8:39. doi:10.1186/1471-2164-8-39

Lee, E.R., J. Trasler, S. Dwivedi, and C.P. Leblond. 1982. Division of the mouse gastric mucosa into zymogenic and mucous regions on the basis of gland features. *Am. J. Anat.* 164:187–207. doi:10.1002/aja.1001640302

Murata, T., K. Furushima, M. Hirano, H. Kiyonari, M. Nakamura, Y. Suda, and S. Aizawa. 2004. *ang* is a novel gene expressed in early neuroectoderm, but its null mutant exhibits no obvious phenotype. *Gene Expr. Patterns.* 5:171–178. doi:10.1016/j.modgep.2004.08.007

Nishikura, K. 2010. Functions and regulation of RNA editing by ADAR deaminases. *Annu. Rev. Biochem.* 79:321–349. doi:10.1146/annurev-biochem-060208-105251

Platani, M., and A.I. Lamond. 2008. Nuclear organisation and subnuclear bodies. *In* RNA Trafficking and Nuclear Structure Dynamics. Springer-Verlag, Berlin. 1–22.

Prasanth, K.V., and D.L. Spector. 2007. Eukaryotic regulatory RNAs: an answer to the 'genome complexity' conundrum. *Genes Dev.* 21:11–42. doi:10.1101/gad.1484207

Prasanth, K.V., S.G. Prasanth, Z. Xuan, S. Hearn, S.M. Freier, C.F. Bennett, M.Q. Zhang, and D.L. Spector. 2005. Regulating gene expression through RNA nuclear retention. *Cell.* 123:249–263. doi:10.1016/j.cell.2005.08.033

Saha, S., S. Murthy, and P.N. Rangarajan. 2006. Identification and characterization of a virus-inducible non-coding RNA in mouse brain. *J. Gen. Virol.* 87:1991–1995. doi:10.1099/vir.0.81768-0

Sasaki, Y.T.F., T. Ideue, M. Sano, T. Mituyama, and T. Hirose. 2009. MENepsilon/beta noncoding RNAs are essential for structural integrity of nuclear paraspeckles. *Proc. Natl. Acad. Sci. USA.* 106:2525–2530. doi:10.1073/pnas.0807899106

Shimoyama, Y., and S. Hirohashi. 1991. Expression of E- and P-cadherin in gastric carcinomas. *Cancer Res.* 51:2185–2192.

Shirayoshi, Y., A. Nose, K. Iwasaki, and M. Takeichi. 1986. N-linked oligo-saccharides are not involved in the function of a cell-cell binding glyco-protein E-cadherin. *Cell Struct. Funct.* 11:245–252. doi:10.1247/csf.11.245

Sone, M., T. Hayashi, H. Tarui, K. Agata, M. Takeichi, and S. Nakagawa. 2007. The mRNA-like noncoding RNA Gomafu constitutes a novel nuclear domain in a subset of neurons. *J. Cell Sci.* 120:2498–2506. doi:10.1242/jcs.009357

Souquere, S., G. Beauclair, F. Harper, A. Fox, and G. Pierron. 2010. Highly ordered spatial organization of the structural long noncoding NEAT1 RNAs within paraspeckle nuclear bodies. *Mol. Biol. Cell.* 21:4020–4027. doi:10.1091/mbc.E10-08-0690

Sunwoo, H., M.E. Dinger, J.E. Wilusz, P.P. Amaral, J.S. Mattick, and D.L. Spector. 2009. MEN epsilon/beta nuclear-retained non-coding RNAs are up-regulated upon muscle differentiation and are essential components of paraspeckles. *Genome Res.* 19:347–359. doi:10.1101/gr.087775.108

Tripathi, V., J.D. Ellis, Z. Shen, D.Y. Song, Q. Pan, A.T. Watt, S.M. Freier, C.F. Bennett, A. Sharma, P.A. Bubulya, et al. 2010. The nuclear-retained noncoding RNA MALAT1 regulates alternative splicing by modulating SR splicing factor phosphorylation. *Mol. Cell.* 39:925–938. doi:10.1016/j.molcel.2010.08.011

Visa, N., F. Puvion-Dutilleul, J.P. Bachellerie, and E. Puvion. 1993. Intranuclear distribution of U1 and U2 snRNAs visualized by high resolution in situ hybridization: revelation of a novel compartment containing U1 but not U2 snRNA in HeLa cells. *Eur. J. Cell Biol.* 60:308–321.

Yagi, T., T. Tokunaga, Y. Furuta, S. Nada, M. Yoshida, T. Tsukada, Y. Saga, N. Takeda, Y. Ikawa, and S. Aizawa. 1993. A novel ES cell line, TT2, with high germline-differentiating potency. *Anal. Biochem.* 214:70–76. doi:10.1006/abio.1993.1458

Zhao, R., M.S. Bodnar, and D.L. Spector. 2009. Nuclear neighborhoods and gene expression. *Curr. Opin. Genet. Dev.* 19:172–179. doi:10.1016/j.gde.2009.02.007